Underwater Light

Curtis D. Mobley

7.1 Introduction

The penetration of the sun's energy into natural waters (oceans, lakes, and rivers) is dependent upon the incident solar radiation, the state of the windblown surface, the bottom reflectance in shallow waters, and the absorbing and scattering properties of the water body. The absorbing and scattering properties are themselves determined by the type, concentration, and size distribution of the dissolved and particulate material within the water. The concentrations of water constituents such as phytoplankton, mineral particles, and dissolved substances vary by many orders of magnitude, and consequently so do absorption and scattering and the resulting measures of underwater light. This chapter introduces the terminology used to describe light and the medium through which it passes, and it illustrates the ranges of values found in natural waters. The emphasis is on the variability of light fields in natural waters.

The recent text by Johnsen (2012) gives an excellent introduction to light written with the needs of biologists in mind. Kirk (1994) discusses aquatic photosynthesis in detail. Mobley (1994) gives an overview of optical oceanography and the mathematics of radiative transfer theory as needed to compute underwater light fields. A good online resource is the Ocean Optics Web Book (www.oceanopticsbook.info).

The quantities needed to describe light and its interactions with water are grouped into three classes: radiometric variables, which describe the light itself; inherent optical properties, which describe material media; and apparent optical properties, which are a combination of the two. The next sections discuss each of these in turn.

C.D. Mobley
Sequoia Scientific, Inc., Bellevue, WA, USA
e-mail: curtis.mobley@sequoiasci.com

7.2 Radiometric Variables

All electromagnetic radiation—light in particular—is fully specified by the four-component Stokes vector, which relates the electric field of the propagating radiation to its state of polarization, spectral distribution of energy, and direction of travel. Many aquatic photobiological processes such as photosynthesis are assumed to be independent of the polarization state, although there may be exceptions such as the possible use of polarized light for navigation or visibility enhancement in searching for prey. This article ignores the complexities of polarization, in which case only the magnitude of the radiant energy is relevant. This is given by the first component of the Stokes vector, which is called the spectral radiance L. To a good approximation, water bodies are often horizontally homogeneous on scales of 100 m or less, in which case the radiance is a spatial function only of the depth z, the polar (θ) and azimuthal (ϕ) directions, and wavelength λ. With these assumptions, the radiance distribution $L(z, \theta, \phi, \lambda)$ gives a complete description of the light field. (Depth z is normally measured positive downward from 0 at the mean water surface; θ and ϕ refer to the direction the light is traveling, with $\theta = 0$ in the $+z$ direction.) Spectral radiance has units of watts of radiant power per unit area (perpendicular to the direction of travel) per unit steradian (of solid angle about direction θ, ϕ), per unit wavelength interval, or W m^{-2} sr^{-1} nm^{-1}. The directional information contained in the radiance is crucial for applications such as prediction of underwater visibility. However, this directional information is not needed for photobiology because absorption by randomly oriented phytoplankton and other water constituents does not depend on the direction of light travel. Thus, the radiometric variables most commonly measured and used for biology and thermodynamics (i.e., water heating) are various irradiances, which are integrals of the radiance over direction.

Consider an instrument with a flat collecting surface, with each point of the surface being equally sensitive to light incident onto the surface from any direction seen by the detector. The detector is equipped with filters so that the incident power is measured as a function of wavelength. If such a detector has its collecting surface pointing upward, so as to collect light traveling downward, it measures the downwelling spectral plane irradiance $E_d(z, \lambda)$, which has units of W m^{-2} nm^{-1}. Note that the effective collection area of the detector as seen by radiance traveling in direction θ relative to the normal to the detector surface reduced by a factor of $\cos\theta$; such instruments are therefore called cosine detectors. If the radiance is known, $E_d(z, \lambda)$ is obtained by integrating the radiance over all downward directions, with the radiance weighted by $\cos\theta$ to account for the sensor angular response:

$$E_{\mathrm{d}}(z,\lambda) = \int\limits_{0}^{\pi/2} \int\limits_{0}^{2\pi} L(z,\theta,\phi,\lambda)\cos\theta\sin\theta\,\mathrm{d}\theta\,\mathrm{d}\phi. \quad (7.1)$$

Here $\sin\theta\,\mathrm{d}\theta\,\mathrm{d}\phi$ is the differential element of solid angle. If the same detector is pointing downward, it measures the upwelling plane irradiance $E_u(z, \lambda)$.

If the detector has a spherical collecting surface (think of a ping pong ball), it is equally able to detect light traveling in any direction. The measured quantity is then the scalar irradiance $E_0(z, \lambda)$, which is obtained from the radiance by integrating over all directions, but without the cosine weighting:

$$E_0(z,\lambda) = \int\limits_{0}^{\pi} \int\limits_{0}^{2\pi} L(z,\theta,\phi,\lambda)\sin\theta\,\mathrm{d}\theta\,\mathrm{d}\phi. \quad (7.2)$$

Scalar irradiance (sometimes called fluence rate by biologists) is the measure of light energy available to drive photobiological processes, which do not depend on the direction of light propagation. Although the probability of a photon being absorbed by a chlorophyll molecule depends on wavelength, all photons, once absorbed, lead to the same photosynthetic reaction. Thus, it is the number of photons absorbed, not their individual energies, that is relevant to primary production calculations. The corresponding radiometric variable is the scalar irradiance converted from energy units (W m^{-2} nm^{-1}) to quantum units (photons s^{-1} m^{-2} nm^{-1}). A single photon contains energy hc/λ, where $h = 6.626\cdot10^{-34}$ J s is Planck's constant, $c = 2.998\cdot10^8$ m s^{-1} is the speed of light, and λ is the wavelength (here in meters).

Thus, the conversion from energy to quantum units is done by multiplying E_0 by λ/hc. A crude but commonly used measure of the total number of photons available for photosynthesis is the photosynthetically available radiation (PAR), defined by

$$\mathrm{PAR}(z) = \int\limits_{400}^{700} E_0(z,\lambda)\frac{\lambda}{hc}\,\mathrm{d}\lambda. \quad (7.3)$$

(Some researchers use 350 nm as the lower bound for the PAR range of wavelengths.) In aquatic systems PAR is often measured in µmol photons m^{-2} s^{-1}, where 1 mol is $6.023\cdot10^{23}$ photons. Note that PAR always refers to quantum units; it is not a synonym for broadband irradiance in energy units.

For studies concerned with the influence of ultraviolet (UV) radiation on aquatic organisms, other broadband quantities are of interest. UV-A is electromagnetic radiation with wavelengths in the 315–400 nm range, and UV-B is radiation in the 280–315 nm range. Thus, for example, the solar scalar irradiance penetrating to depth within the UV-B region of the spectrum, $E_{\mathrm{UV\text{-}B}}(z)$, is computed as

$$E_{\mathrm{UV\text{-}B}}(z) = \int\limits_{280}^{315} E_0(z,\lambda)\,\mathrm{d}\lambda. \quad (7.4)$$

There are other radiometric variables, but these give us what is needed.

7.3   Inherent Optical Properties

The optical properties of a material medium—here a water body—are specified by its inherent optical properties (IOPs). IOPs depend only on the medium, not on the light propagating through it. The two fundamental IOPs are the spectral absorption coefficient, $a(\lambda)$, and the volume scattering function $\beta(\psi, \lambda)$, where ψ is the scattering angle measured from 0 in the forward (unscattered) direction of light propagation. These two quantities fully specify (ignoring polarization) how light can interact with the medium.

Consider monochromatic light propagating in a particular direction through a water body. In going from location r to $r+\Delta r$ along the direction of propagation, some amount $\Delta\Phi(r)$ of the incident power $\Phi(r)$ is absorbed by the water. The fraction of power absorbed is the absorptance $A = \Delta\Pi(r)/\Pi(r)$. All quantities depend on wavelength, but not on the direction of propagation (in isotropic media such as water). The absorption coefficient $a(\lambda)$ is the absorptance per unit distance traveled, or conceptually

$$a = \lim_{\Delta r \to 0} \frac{\Delta\Phi(r)}{\Phi(r)\Delta r} = \frac{\mathrm{d}\ln\Phi(r)}{\mathrm{d}r}, \quad (7.5)$$

with units of m^{-1}. Radiant energy absorbed at one wavelength is converted to chemical or thermal energy or is reemitted at another wavelength by fluorescence or other inelastic processes.

Rather than being absorbed, the radiant power may be scattered, i.e., the direction of propagation (elastic scattering) and or wavelength (inelastic scattering) may change through interaction with the water. The volume scattering function (VSF) is the fraction of incident power scattered into a unit solid angle centered on direction (ψ, α) per unit distance traveled. Here ψ is the polar scattering angle measured from zero in the direction of the unscattered beam, and α is the azimuthal angle of the scattering. If $\Delta\Phi_s$ is the power scattered into solid angle $\Delta\Omega$ as the light travels distance Δr, then the VSF is conceptually defined as

$$\beta(\psi, \alpha) = \lim_{\Delta r \to 0} \lim_{\Delta\Omega \to 0} \frac{\Delta\Phi_s(\psi, \alpha)}{\Phi\Delta r \cdot \Delta\Omega}, \qquad (7.6)$$

with units of m^{-1} sr^{-1}. For unpolarized light and isotropic media, as assumed here, scattering depends only on ψ.

Equations 7.5 and 7.6 are the definitions of these IOPs. Actual instruments of course have finite path lengths and solid angles. Moreover, the actual measurement of a and β are complicated by the fact that both absorption and scattering are always present, often in roughly equal amounts, in any water body. Thus, an instrument measuring the absorption coefficient must be corrected for losses from the incident beam due to scattering, which would otherwise appear as increased absorption. Likewise, a measurement of scattering must be corrected for absorption losses from the incident beam. A vicious circle thus results, which is the bane of IOP measurements in natural waters with both absorbing and scattering constituents.

IOPs are additive. That is, the total a and β are the sums of contributions by pure water, phytoplankton, mineral particles, dissolved substances, air bubbles, etc. This allows a and β for various water constituents to be measured or modeled separately. There are many such biogeochemical models for a and β for specific kinds of particles and dissolved substances. These models often parameterize the IOPs in terms of more easily measured quantities, e.g., absorption by phytoplankton is often modeled as a function of the chlorophyll concentration.

Just as for radiance, the angular scattering information contained in the VSF provides more information than is necessary for photobiological applications (although it is crucial for other applications such as remote sensing and visibility). The scattering coefficient b gives a measure of the total amount of scattering, without regard for the direction of the scattered radiance, and is obtained by integrating the VSF over all scattering directions (ψ, α):

$$b = \int_0^{2\pi}\int_0^{\pi}\beta(\psi, \alpha)\sin\psi\, d\psi\, d\alpha = 2\pi\int_0^{\pi}\beta(\psi)\sin\psi\, d\psi. \quad (7.7)$$

b has units of m^{-1}. The 2π in the last term results from the assumption that the scattering is azimuthally symmetric so that the VSF is independent of α. The scattering phase function $\tilde{\beta}(\psi)$ is the VSF normalized by the total scattering coefficient:

$$\tilde{\beta}(\psi, \lambda) = \frac{\beta(\psi, \lambda)}{b(\lambda)}, \qquad (7.8)$$

which has units of sr^{-1}. The phase function thus shows the angular shape of the VSF without regard to the magnitude of the scattering.

The total loss of power from a collimated beam owing to both absorption and scattering out of the beam is given by the beam attenuation coefficient, $c = a + b$. The backscatter coefficient b_b is given by the VSF integrated over all scattering directions greater than 90°, i.e., over $\pi/2$ to π in Eq. 7.7. The ratio of b_b/a is a fundamental parameter for predicting how much radiance incident onto the sea surface is scattered back upward and returned to the sky without being absorbed. That water-leaving radiance is sunlight that has been transformed by interaction with the water column and thus carries information about the biogeochemical state of the water body. The backscatter fraction b_b/b is sensitive to particle size and index of refraction and thus carries information about the type of scattering particles in the water.

Case 1 waters are those in which the IOPs are determined predominantly by phytoplankton and their covarying derivatives (detritus from dead cells and colored dissolved organic matter (CDOM) released by the cells). In such waters, absorption and scattering are correlated and can be parameterized by the chlorophyll concentration (albeit with large variability owing to phytoplankton physiological state and cell size for a given chlorophyll value). However, in general, absorption and scattering are uncorrelated and cannot be modeled by chlorophyll concentration alone. Consider, for example, coastal water containing high concentrations of CDOM from land runoff or sand from resuspended sediment. CDOM is strongly absorbing but almost nonscattering, whereas quartz sand is highly scattering but almost nonabsorbing. Such waters are called case 2. Both absorption and scattering are equally important in understanding underwater light, and both must be measured.

Figure 7.1 shows the range of absorption and scattering coefficients as a function of chlorophyll concentration in case 1 water according to the bio-optical models of Bricaud et al. (1998) for $a(\lambda)$ and Morel et al. (2002) for $b(\lambda)$. The left panel shows that the absorption coefficient varies by over two orders of magnitude at blue wavelengths over the range of the clearest ocean water (Chl = 0.01 mg m^{-3}) to extreme bloom conditions (Chl = 100 mg m^{-3}). The right panel shows that the scattering coefficient varies by five orders of magnitude for the same range of chlorophyll values. The actual

Fig. 7.1 Modeled variability of absorption and scattering coefficients in case 1 water as a function of chlorophyll concentration. The curves in each panel from bottom to top are for pure water, Chl = 0.01, 0.1, 1, 10, and 100 mg m^{-3}
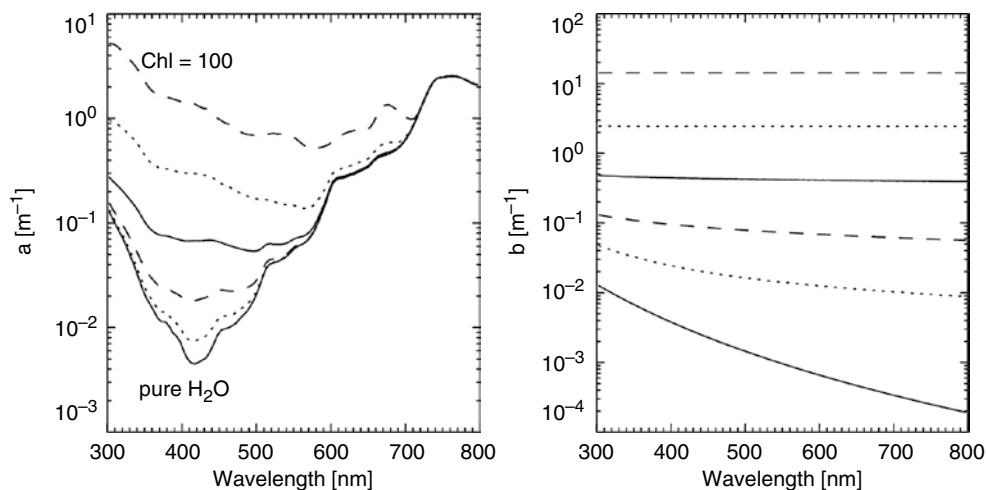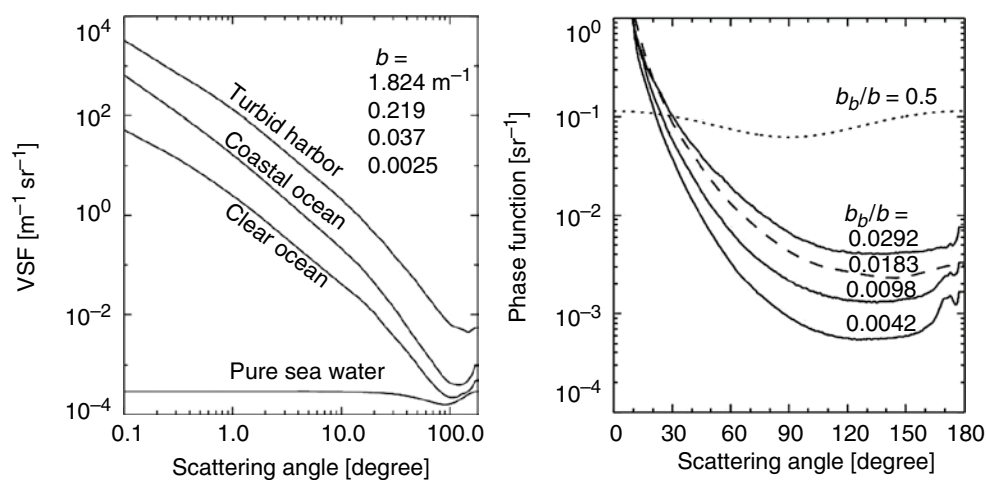
Fig. 7.2 Example variability in measured VSFs (*left panel*) and phase functions (*right panel*)

variability in both magnitude and spectral shape is much greater because of contributions by CDOM, mineral particles, microbubbles, and other water components that are often present in natural waters.

Variability in VSFs is just as great. The left panel of Fig. 7.2 shows three VSFs measured (Petzold 1972) at 514 nm (with an instrument with a 75 nm bandwidth) in clear Bahamas water, coastal California, USA, water, and the turbid harbor at San Diego, California, USA. There is a factor of 60 difference in the magnitudes of the clear versus turbid VSFs at small scattering angles, and each VSF has over five orders of magnitude difference between scattering angles of 0.1° and 180°. The corresponding total scattering coefficients vary by a factor of 50. The bottom curve of that figure shows the VSF for pure seawater. It is negligible in magnitude compared to the other VSFs, except at backscatter directions for the clearest ocean water. Backscatter by pure water becomes a significant part of the total backscatter in very clear waters.

The solid lines in the right panel of Fig. 7.2 show three phase functions $\tilde{\beta}(\lambda, 530 \text{ nm})$ measured in coastal New Jersey, USA, surface waters. These measurements were made within 1 day and a few kilometers of each other. Nevertheless, these phase functions differ by almost an order of magnitude in backscatter directions ($\psi > 90°$), and their backscatter fractions b_b/b vary by a factor of seven, from 0.42 % to almost 3 %. The dashed line in this panel shows the phase function for the Petzold San Diego harbor VSF, and the dotted line is the phase function for pure seawater. Pure seawater scatters symmetrically about $\psi = 90°$ and thus has a backscatter fraction of 0.5.

7.4   Apparent Optical Properties

As noted, the radiance distribution tells us everything there is to know about light, and the total IOPs $a(z, \lambda)$ and $b(\psi, z, \lambda)$ tell us everything about the optical properties of a water body. The behavior of radiance in a water body can be accu-

rately predicted by solving the radiative transfer equation (RTE), which expresses conservation of energy in terms of radiance. The inputs to the RTE are the total IOPs throughout the medium, the external radiance incident onto the water surface, the surface wave state (usually parameterized by the wind speed), and, for finitely deep water, the depth and reflectance of the bottom. The RTE is a very complicated integrodifferential equation and must be solved numerically. There are many techniques to do this (Mobley et al. 1993), and commercial software is available and widely used for solving the RTE in the aquatic setting (by the author and is a commercial product of Sequoia Scientific, Inc.; www.hydrolight.info). The RTE, hence light propagation in the ocean, depends only on the total IOPs. In other words, a photon only cares whether it is absorbed or scattered; what type of molecule does the absorption or scattering is irrelevant to the prediction of light propagation. Biologists, on the other hand, do care how much light is absorbed or scattered by each water column constituent; e.g., light absorbed by a mineral particle or water molecule is not available to be absorbed by a phytoplankton and thereby lead to photosynthesis.

However, as also noted, radiance and IOPs are difficult to measure and in many cases contain more information than is needed. This leads us to search for easily made optical measurements that can tell us something about the biogeochemical state of a water body, but without the need to measure the full radiance distribution or set of IOPs. Apparent optical properties (AOPs) satisfy this need. An ideal AOP depends strongly on the absorbing and scattering properties of the water body (i.e., on its biogeochemical state) but only weakly on external environmental conditions such as the incident solar radiance or surface wave state. Note that irradiance, for example, is not an AOP. It does depend on the water properties, but it is very sensitive to the external environment. For example, if the sun goes behind a cloud, the irradiance can change by an order of magnitude within seconds, even though the water body remains unchanged. An irradiance measurement thus tells us little about the water body itself.

AOPs are usually either ratios or normalized depth derivatives of radiometric variables. One of the most important AOPs is the remote-sensing reflectance, $R_{rs}(\lambda) = L_w(air, \lambda)/E_d(air, \lambda)$ with units of sr^{-1}. $L_w(air, \lambda)$ is the water-leaving radiance measured in air just above the sea surface, and $E_d(air, \lambda)$ is the incident sky and solar irradiance. L_w depends on the water properties because it is radiance that has passed into the water column, there to be modified by the water IOPs, and then been scattered back to the atmosphere. Its magnitude is sensitive to the external environment. However, the normalization of L_w by $E_d(air, \lambda)$ largely removes the effects of the external environment. For example, if E_d decreases by some factor
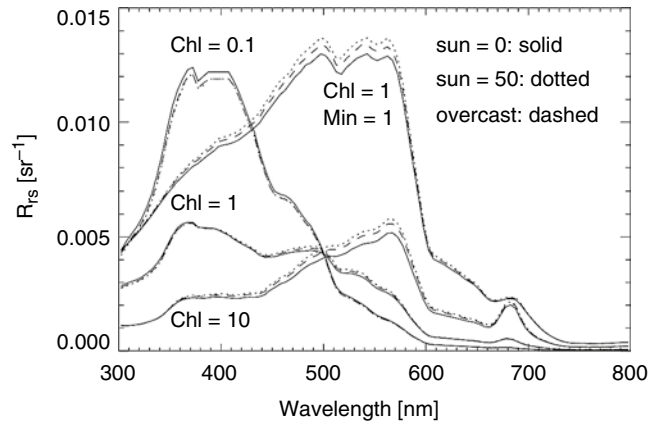

Fig. 7.3 Modeled example dependence of remote-sensing reflectance R_{rs} on water properties and sky conditions

when the sky goes from clear to cloudy, so does the radiance within the water body; hence, L_w decreases by the same factor, and the ratio L_w/E_d remains unchanged except for a small difference due to the different angular distributions of the incident radiance for the cloudy versus clear sky. Figure 7.3 illustrates the dependence of R_{rs} on water and sky conditions. The HydroLight radiative transfer code was used to solve the RTE using IOPs that were parameterized by chlorophyll and mineral particle concentrations for homogeneous water. R_{rs} was obtained from the computed radiance distribution $L(z, \theta, \phi, \lambda)$ using the definitions above. Four sets of IOPs were used: Chl = 0.1, 1, and 10 mg m^{-3} with no mineral particles and Chl = 1 mg m^{-3} with an additional 1 g mm^{-3} of red clay mineral particles. Three sky conditions were used: the sun at zenith angles of 0° and 50° in a clear sky and a heavily overcast sky. The figure shows that the R_{rs} spectra group nicely by water IOPs, with only a small variability caused by the sky condition. R_{rs} is thus a good AOP. Indeed, it is the basis for most satellite ocean color remote sensing, which has revolutionized our understanding of the oceans over the last half century.

Another reflectance AOP is the irradiance reflectance $R = E_u/E_d$. R_{rs} is less sensitive to sky conditions than is R and has thus replaced it as the reflectance most commonly used in remote sensing. R does, however, have the virtue of being measurable by just one instrument: the same cosine detector is used facing downward and then upward to measure E_u and E_d, respectively, which minimizes instrument calibration problems. Indeed, it is not even necessary that the plane irradiance sensor be calibrated to energy units; any multiplicative calibration factor cancels out.

Diffuse attenuation functions comprise another family of AOPs. These AOPs are normalized depth derivatives of radiometric variables. The diffuse attenuation function for downwelling plane irradiance E_d is defined by

$$K_d(z,\lambda) = -\frac{1}{E_d(z,\lambda)}\frac{dE_d(z,\lambda)}{dz} = -\frac{d\ln E_d(z,\lambda)}{dz}, \quad (7.9)$$

with units of m^{-1}. As with R, multiplicative factors on E_d resulting either from environmental changes or instrument calibration cancel. There is a K function for any radiometric variable; K_d, K_o, K_{Lu}, and K_{PAR} are the most commonly used. $L_u(z, \lambda)$ is the underwater radiance traveling toward the zenith. Equation 7.9 can be rewritten as

$$E_d(z,\lambda) = E_d(0,\lambda)\exp\left[-\int_0^z K_d(z',\lambda)dz'\right]. \quad (7.10)$$

Here $E_d(0, \lambda)$ is the irradiance just below the air-water surface. If K_d can be measured or modeled, E_d can be computed for a given surface irradiance value without solving the RTE. Similar equations hold for other K functions.

Near the sea surface, K functions depend on depth even in homogeneous water. This is because the angular distribution of the radiance distribution changes with depth as scattering redistributes the directional pattern of the incident sky radiance after it enters the water. However, in homogeneous water all K functions for a given set of IOPs approach a common value at great depth. This asymptotic K value, K_∞, is determined only by the IOPs. Other AOPs also approach asymptotic values and become IOPs at great depth. The asymptotic values can be computed from radiative transfer theory, given the IOPs. The rate at which AOPs approach their asymptotic values depends on the relative amount of absorption and scattering in the water. Higher scattering redistributes the angular pattern of the radiance quicker, so AOPs become asymptotic at shallower depths in highly scattering water than in highly absorbing water. These behaviors are illustrated in Fig. 7.4. HydroLight was again used to compute underwater radiances, from which K_d, K_{Lu}, and K_o were computed from their definitions. The simulations used IOPs for case 1 water with chlorophyll concentrations of Chl = 1 and 5 mg m^{-3} and clear sky conditions with solar zenith angles of 0° and 60°. For given IOP and sky conditions, the three K functions have different values near the sea surface, but they approach a common K_∞ value at depth. For a given chlorophyll value, the K functions near the surface depend on the sky condition. The K functions for the two different chlorophyll values separate at depth and become independent of sky condition. Note that the functions for the Chl = 5 mg m^{-3} approach their asymptotic value at a shallower depth than the curves for Chl = 1. This is because the higher scattering for the higher chlorophyll water redistributes the angular pattern of the radiance distribution more quickly with depth.
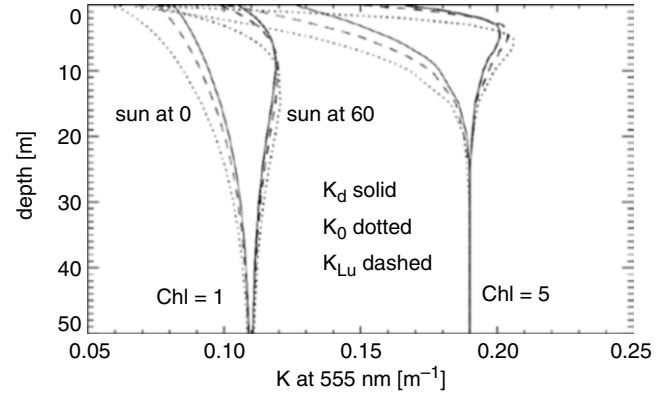

Fig. 7.4 Example dependence of diffuse attenuation functions at 555 nm on water and sky conditions. For each chlorophyll value, the three curves to the left near the surface are for the sun at the zenith, and the curves to the right are for a sun zenith angle of 60°. K_∞(Chl = 1) = 0.11 m^{-1} and K_∞(Chl = 5) = 0.19 m^{-1}

IOPs do not depend on the ambient radiance and therefore can be measured on water samples. AOPs on the other hand do depend on the radiance and therefore must be measured in situ.

7.5 Variability of Underwater Irradiance

Natural waters vary enormously in composition. The clearest ocean or lake waters may have phytoplankton chlorophyll concentrations as low as 0.01 mg m^{-3}. At the other extreme, highly eutrophic lakes can have chlorophyll concentrations over 1,000 mg m^{-3}. Typical oceanic chlorophyll values are in the 0.1–10 range, with 0.5 being a rough global average. Water can contain almost no mineral particles, or a river can carry sediment loads of over 1 kg m^{-3}. Mineral particles can be highly absorbing, especially at blue wavelengths, or non-absorbing quartz or calcite particles. Scattering is strongly affected by the particle size distribution for a given type of particle. (As an analogy, think of the low visibility resulting from scattering by many small fog droplets versus much better visibility through fewer large rain drops, even though the water mass per cubic meter is the same.) The same variability holds for dissolved substances, not to mention pollutants. These wide ranges of water constituent types and concentrations produce an equally wide range in the magnitudes and spectral shapes underwater light fields.

Figure 7.5 shows HydroLight-computed examples of spectral scalar irradiance $E_o(z, \lambda)$ in quantum units in case 1 water for chlorophyll values of 0.01, 1, and 100 mg m^{-3}. Note that the wavelength of maximum light penetration shifts from deep blue at Chl = 0.01 to green at Chl = 1 to yellow at Chl = 100.
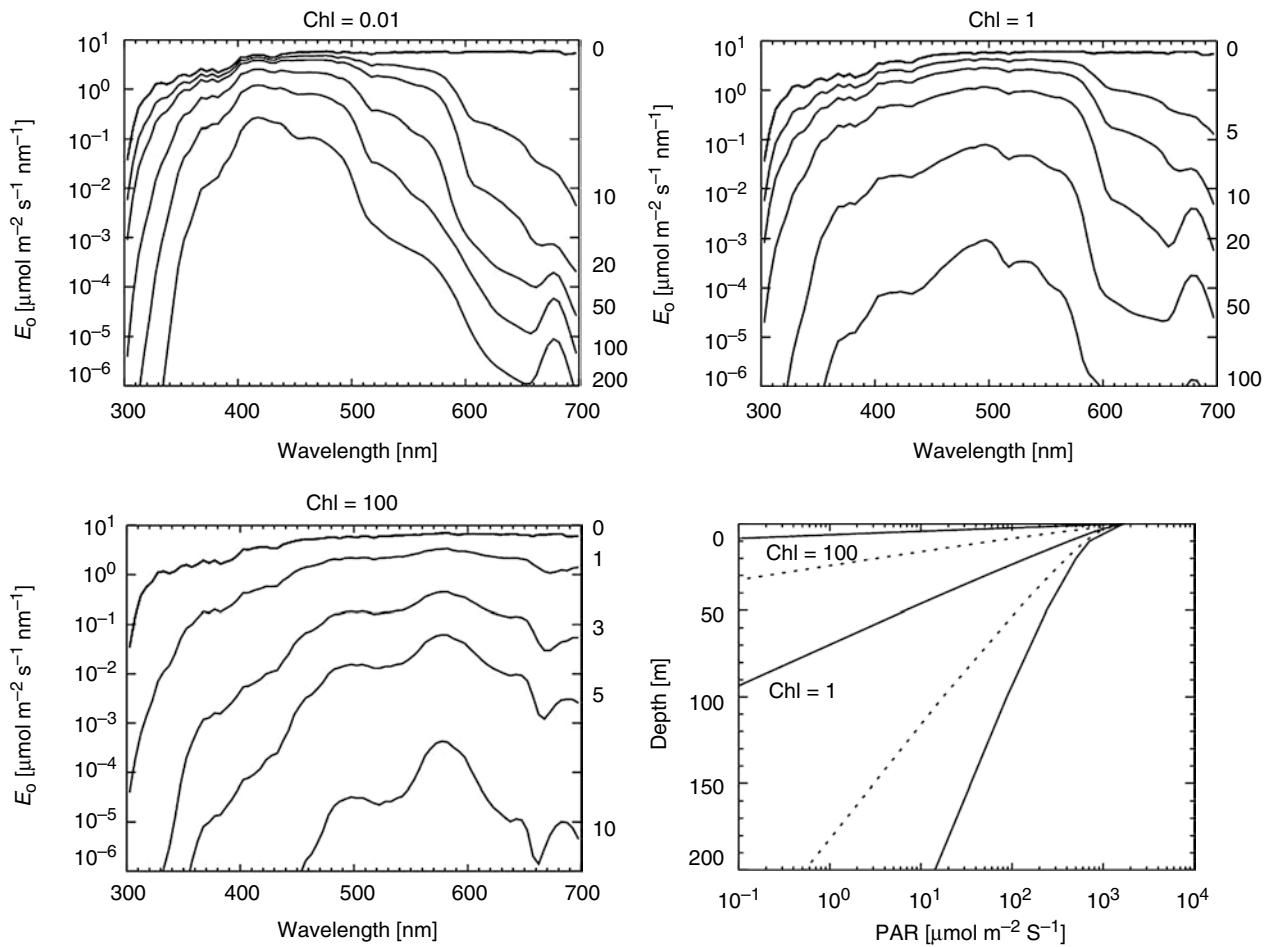
Fig. 7.5 Computed examples of spectral scalar irradiance E_0 in quantum units for chlorophyll values of 0.01, 1, and 100 mg m^{-3}. The numbers to the right of these plots show the depth in meters of the plotted spectra. The *solid lines* in the lower right panel shows the corresponding PAR values (computed from 400 to 700 nm); the *dashed lines* are for Chl = 0.1 and 10 mg m^{-3}

This wavelength dependence allows different species of phytoplankton, which have different pigment suites, to have a competitive advantage in different types of water. For this reason, the latest generation of ocean ecosystem models (Bissett et al. 1999) uses spectral irradiance rather than PAR to drive primary production calculations. The lower right panel of Fig. 7.5 shows the PAR values corresponding to the chlorophyll values of the other panels; dotted lines are for intermediate chlorophyll values. A rough rule of thumb says that photosynthesis can occur to PAR values as low as 1 μmol photons m^{-2} s^{-1}. This rule and these simulations indicate that photosynthesis occurs as deep as several hundred meters in the clearest water, but to only a few meters in very eutrophic water. The values in this figure were computed for the sun at a solar zenith angle of 50° in a clear sky; the values scale almost directly with changes in incident irradiance onto the sea surface for different sky conditions.

The simulations and data shown above only hint at the nature and variability of underwater light fields. The variety of water constituents is almost endless. Different species of phytoplankton have much different absorbing and scattering properties, which depend in complicated ways on the plankton light history and nutrient availability and thus show large variability even for the same species. The same holds for different types of mineral particles and dissolved substances. The types and concentrations of these components are often uncorrelated and vary widely with geographic location, time, and depth. The end result is that the underwater optical environment can be almost anything from the clearest of waters in which light penetrates hundreds of meters to almost opaque waters that become dark less than a meter below the surface. These differences in light environments are reflected in the much different biological communities in the world's waters.

References

Bissett WP, Carder KL, Walsh JJ, Dieterle DA (1999) Carbon cycling in the upper waters of the Sargasso Sea: II. Numerical simulation of apparent and inherent optical properties. Deep-Sea Res I 46:271–317

Bricaud A, Morel A, Babin M, Allali K, Claustre H (1998) Variations of light absorption by suspended particles with chlorophyll a concentration in oceanic (case 1) waters: analysis and implication for bio-optical models. J Geophys Res 103(C13):31033–31044

Johnsen S (2012) The optics of life: a biologist's guide to light in nature. Princeton University Press, Princeton

Kirk JTO (1994) Light and photosynthesis in aquatic ecosystems. Cambridge University Press, Cambridge

Mobley CD (1994) Light and water: radiative transfer in natural waters. Academic, San Diego (out of print but available on CD from the author or online at www.oceanopticsbook.info)

Mobley CD, Gentili B, Gordon HR, Jin Z, Kattawar GW, Morel A, Reinersman P, Stamnes K, Stavn R (1993) Comparison of numerical models for the computation of underwater light fields. Appl Optics 32(36):7484–7504

Morel A, Antoine D, Gentili B (2002) Bidirectional reflectance of oceanic waters: accounting for Raman emission and varying particle scattering phase function. Appl Optics 41(30):6289–6306

Petzold TJ (1972) Volume scattering functions for selected ocean waters. SIO Ref. 72–78, Scripps Inst. Oceanogr., 79 pages